



# Hydraulic properties of individual xylem vessels of *Fraxinus americana*

Maciej A. Zwieniecki<sup>1</sup>, Peter J. Melcher and N. Michele Holbrook

Department of Organismic and Evolutionary Biology, Biological Laboratories, Harvard University, 16 Divinity Ave, Cambridge, MA 02138, USA

Received 8 May 2000; Accepted 6 September 2000

## Abstract

Studies of the hydraulic properties of xylem vessels have been limited to measurements of whole plant or whole stem segments. This approach allows the longitudinal transport properties of the ensemble of vessels within a stem to be determined, but provides little information on radial transport. Here the xylem of *Fraxinus americana* L. has been examined using a new method that allows the transport properties of individual vessels to be examined. One goal of this study was to quantify transport parameters relevant to embolism repair. The longitudinal conductivity of vessel segments open at both ends (i.e. no end walls) agreed with values predicted by the Poiseuille equation. Radial specific conductance (conductance per unit area) was approximately six orders of magnitude lower than the longitudinal conductance of the vessel segment normalized by the cross-sectional area of the vessel lumen. There was a step increase in the radial specific conductance of previously gas-filled vessels when the delivery pressure exceeded 0.4 MPa. This is consistent with the idea that positive pressure, required for embolism repair, can be compartmentalized within a vessel if the bordered pit chambers are gas-filled. The diffusion coefficient for the movement of gas from a pressurized air-filled vessel was of the same order of magnitude as that for air diffusing through water ( $1.95 \text{ e}^{-9} \text{ m}^2 \text{ s}^{-1}$ ). Estimates of the time needed to displace all of the gas from an air-filled vessel were in the order of 20 min, suggesting that gas removal may not be a major limitation in embolism repair.

Key words: Hydraulic conductivity, xylem vessel, *Fraxinus americana* L., Poiseuille equation, embolism.

## Introduction

Current understanding of the hydraulic properties of vascular plants is based primarily on measurements of water flow through excised stem, root and branch segments (Zimmermann, 1983; Tyree and Ewers, 1991; Sperry *et al.*, 1993; Jarbeau *et al.*, 1995; Alder *et al.*, 1996; Sperry and Ikeda, 1997; but see Giordano *et al.*, 1978). The standard approach is to determine the conducting capacity of the ensemble of vascular conduits within the measured segment and thus the ability of the measured segment to supply downstream regions of the plant with water (Sperry *et al.*, 1988a). The hydraulic conductivity of an individual segment may change with time due to the cavitation of xylem conduits and any subsequent refilling (Waring and Running, 1978; Milburn, 1979; Sperry, 1986; Sperry *et al.*, 1988b; Pickard, 1989; Tyree and Yang, 1992; Edwards *et al.*, 1994; Cochard *et al.*, 1994; Magnani and Borghetti, 1995; Zwieniecki and Holbrook, 1998). Because cavitation and embolism repair take place at the level of individual vessels, understanding dynamic changes in conductivity requires methods that address the hydraulic properties of individual conduits. Over the past years, a number of techniques (e.g. double staining, cryo-scanning electron microscopy, magnetic resonance imaging) have been introduced to examine the functional state of individual xylem vessels (Canny, 1997; Kockenberger *et al.*, 1997; Zwieniecki and Holbrook, 1998; Tyree *et al.*, 1999). In this paper, the longitudinal conductivity and radial specific conductance of early-wood vessels of *Fraxinus americana* L. (white ash) are examined using a new approach that allows the examination of the hydraulic properties of single vessels. This work is motivated, in part, by observations of short-term (diurnal) fluctuations in hydraulic conductivity of *F. americana* branches (Zwieniecki and Holbrook, 1998). Because the mechanism allowing increases in conductivity is not well understood, the ability of conduits to contain positive

<sup>1</sup> To whom correspondence should be addressed. Fax: +1 617 496 5854. E-mail: mzwienie@oeb.harvard.edu

pressures was examined and the factors limiting rates of gas removal from embolized vessels were quantified.

The ability to refill embolized vessels has long been recognized in plants that exhibit root pressure (O'Leary, 1965; Zimmermann and Brown, 1971; Milburn and McLaughlin, 1974; Milburn, 1979; Putz, 1983; Sperry *et al.*, 1988a, b; Pickard, 1989; Cochard *et al.*, 1994; Sperry and Ikeda, 1997). Recent studies, however, have demonstrated diurnal changes in stem hydraulic conductance without the pressurization of the entire xylem (Salleo *et al.*, 1996; Zwieniecki and Holbrook, 1998; Tyree *et al.*, 1999; Zwieniecki *et al.*, 2000), suggesting that refilling may also occur by a more localized mechanism (Holbrook and Zwieniecki, 1999). In either case, positive pressures are needed to force the gas into solution, whereas gas removal depends on factors limiting transport through surrounding tissues. Quantifying the ease with which both water and air can exit radially from an individual vessel will thus contribute to an understanding of embolism repair. Knowing the radial permeability to water will help in understanding the degree to which individual vessels can contain positive pressures, while measurements of the lateral gas permeability through the stem can be used in determining factors limiting rates of gas removal. A theoretical model of embolism reversal (Yang and Tyree, 1992) indicated that from 2–200 h might be needed to refill a completely air-filled vessel, where the estimated time is a function of vessel diameter, distance to edge of stem, and pressure within the refilling vessel. The longest of these estimates is clearly at variance with the suggestion that embolisms may be repaired over a period of several hours, underscoring the need to characterize the movement of gas from individual vessels empirically.

The ability to repair embolisms while much of the xylem is under tension requires a mechanism for compartmentalizing positive pressures within a single vessel (Holbrook and Zwieniecki, 1999). These authors also suggest that a sealing mechanism could result from the formation of a convex gas:water interface within inter-vessel pits (Zwieniecki and Holbrook, 2000). Because the force arising from surface tension due to the curvature of this meniscus opposes any positive pressures developed within the refilling vessel, it could sustain the pressure difference between the refilling vessel (positive pressure) and adjacent conduits (negative pressure). The ability to examine the hydraulic behaviour of single vessels allows this proposed sealing mechanism to be tested. Specifically, by measuring the steady-state rate at which water is pushed into a gas-filled vessel as a function of applied pressure, it can be determined if there is a minimum 'threshold' pressure needed to force water across the perimeter of the vessel and also whether this pressure is consistent with values calculated from the predicted curvature of the gas:water interface (Zwieniecki and Holbrook, 2000).

## Materials and methods

### Hydraulic conductivity of single vessels

Branches (*c.* 1.0 m in length) from a single 10 m tall white ash tree (*Fraxinus americana* L. Oleaceae) were collected in the morning during winter months (December to January). The hydraulic conductivity of individual xylem vessels was determined on 3–6 cm long branch segments by delivering pressurized water through a microcapillary of known resistance and measuring the mass flux at the downstream end of the branch segment. In summary, the procedure followed was (1) measure microcapillary resistance; (2) attach microcapillary to an individual vessel; (3) determine flow of fluid through the microcapillary–vessel system under a known pressure gradient; and (4) measure vessel dimensions (length and diameter).

Microcapillary tubes were pulled on a horizontal pipette puller (Flaming/Brown P-87, Sutter Instrument Company, Novato, CA) and the glass tips subsequently broken such that the opening ranged from 60–120  $\mu\text{m}$  in diameter (the approximate size of early-wood xylem vessels in 1-year-old ash branches). The hydraulic resistance of each microcapillary was determined by measuring the water flux through the microcapillary at a known pressure gradient. The tip was then inserted into the open lumen of an individual vessel using a 50 $\times$  stereo microscope and a micromanipulator (Fig. 1A) and fixed in place using a low-viscosity, fast-setting acrylic glue (Loctite<sup>®</sup> superbond 407; Fig. 1B). The microcapillary was mechanically stabilized with additional glue (which tended to block the openings of neighbouring vessels; Fig. 1C) or with a glass rod secured to the side of the stem segment (Fig. 1D). Safranin dye was pushed through the microcapillary–vessel system at low pressure (<0.01 MPa) to stain the vessel walls so that the vessel at the opposite end of the stem segment could be located (Figs 1E, 2A). The ability to push water through the vessel at such a low pressure indicated that the vessel was continuous (i.e. no end-walls) within the branch segment. Longitudinal hydraulic conductivity of the microcapillary–vessel system was determined by measuring the flow rate of water at a known pressure gradient. Pressurized water was supplied using a captive air-tank connected with a pressure gauge ( $\pm 0.15$  kPa). All measurements were performed using deionized, filtered (0.2  $\mu\text{m}$ ) water. Flow rates were determined using an analytic balance (Sartorius  $\pm 0.01$  mg) interfaced to a computer. After completing the hydraulic measurements, the length of the branch segment (considered to be equal to the length of the vessel under study,  $l_v$ ) was measured and the major and minor radii of the stained vessel cross-section were measured at three locations along the stem segment. Vessel radius ( $r$ ) was calculated as the average of these six measurements.

### Longitudinal hydraulic conductivity

Vessel longitudinal conductivity ( $L_v$ ;  $\text{m}^4 \text{s}^{-1} \text{MPa}^{-1}$ ; Fig. 2B) was determined from measurements of the volumetric flow rate ( $J$ ;  $\text{m}^3 \text{s}^{-1}$ ) divided by the pressure gradient along the vessel ( $\Delta P_v/l_v$ ;  $\text{MPa m}^{-1}$ ):

$$L_v = \frac{J}{\Delta P_v/l_v} \quad (1)$$

The pressure drop along the vessel ( $\Delta P_v$ ; MPa) was calculated as the product of the volumetric flow rate across the microcapillary–vessel system and vessel resistance  $R_v$ , where  $R_v$  is the difference between the total resistance of the microcapillary–vessel system ( $R_{mv}$ ) and the previously determined resistance of the microcapillary ( $R_m$ ; all resistances in

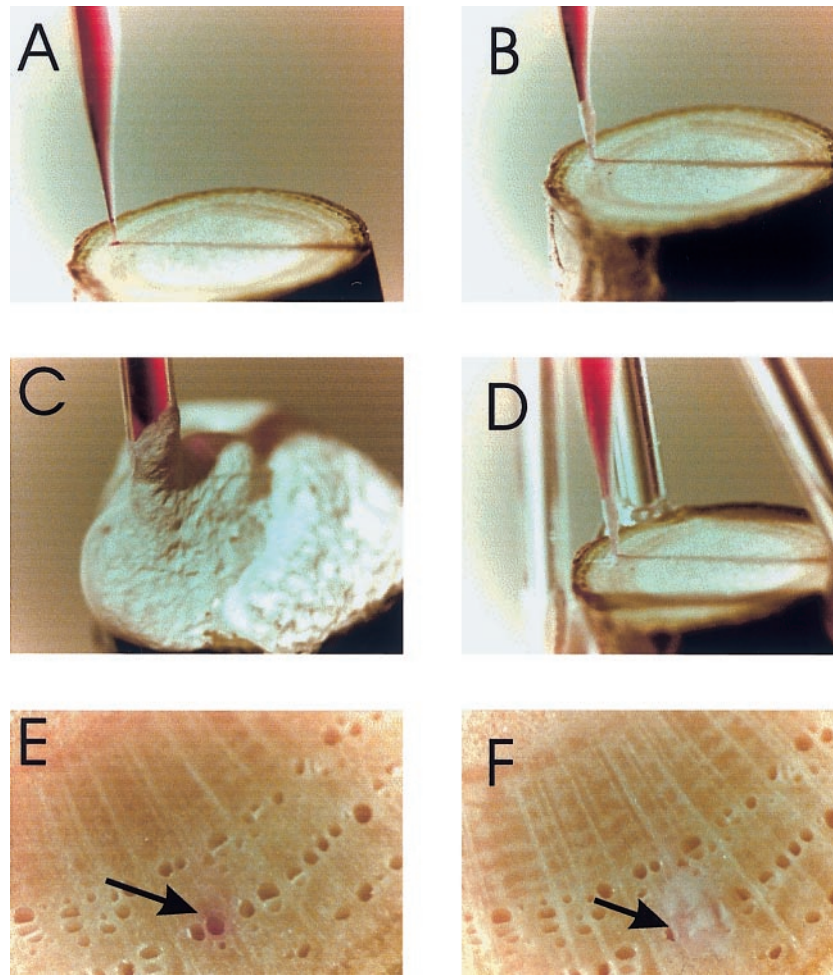


**Fig. 1.** Illustration of steps involved in measuring the hydraulic properties of individual xylem vessels; (A) view of a microcapillary inserted into a vessel; (B) microcapillary sealed into the vessel with acrylic glue; (C) entire end of the stem is covered with glue to provide support for the microcapillary and to block any longitudinal flow (used in longitudinal and radial vessel hydraulic properties determination); (D) supporting structure used to support microcapillary while neighbouring vessels were open for flow (used in the air movement experiments); (E) single vessel stained at the distal end of the stem; (F) droplet of glue used to seal the distal end of a single vessel without blocking the ends of neighbouring vessels.

units of  $\text{MPa s m}^{-3}$ ):

$$\Delta P_v = J(R_{mv} - R_m) = J \left( \frac{\Delta P_{mv}}{J} - R_m \right) \quad (2)$$

$R_{mv}$  was calculated from the measured pressure drop across the microcapillary–vessel system ( $\Delta P_{mv}$ ) divided by the flow rate ( $J$ ). The theoretical conductivity of the vessel ( $L_{th}$ ) was calculated according to the Poiseuille equation:

$$L_{th} = \frac{\pi r^4}{8\eta} \quad (3)$$

where  $\eta$  is the viscosity of water ( $1.002 \text{ e}^{-9} \text{ MPa s}$ ) at  $20^\circ \text{C}$ .

#### Radial specific conductance

Following measurements of longitudinal hydraulic conductivity, the distal end of the stained vessel was carefully sealed with glue such that adjacent vessel openings remained unblocked (Figs 1F, 2C). The microcapillary–vessel system was filled with water and attached to a high-pressure  $\text{N}_2$  tank. The water in the microcapillary–vessel system was then pressurized to 2.5 MPa and the volume flow rate into the vessel was determined by measuring

the time required for the meniscus to move a specified distance along the microcapillary tube. A digital camera was used to record the movement of the meniscus within the microcapillary. The steady-state rate of water movement into the vessel was assumed to equal the flow rate out of the vessel. Following this measurement, the entire distal end of the branch segment was covered with acrylic glue, such that all of the neighbouring vessels were sealed (Fig. 2D). The vessel was then repressurized to 2.5 MPa and the flow measurement repeated.

Because it was not possible to determine the path-length over which radial flow occurred during these measurements, a radial specific conductance was calculated as the rate at which water exits the vessel normalized by area and the applied pressure ( $\text{m}^3 \text{ m}^{-2} \text{ s}^{-1} \text{ MPa}^{-1}$ ):

$$L_r = \frac{J}{\Delta P A_v} \quad (4)$$

where  $\Delta P$  (MPa) is the difference between the pressure applied to the vessel and the outside ambient pressure,  $A_v$  ( $\text{m}^2$ ) is the interior surface area of the vessel, and  $J$  ( $\text{m}^3 \text{ s}^{-1}$ ) is the volume flow rate. Water may exit the vessel through either pit pores or the wall itself, although the latter pathway is likely to have

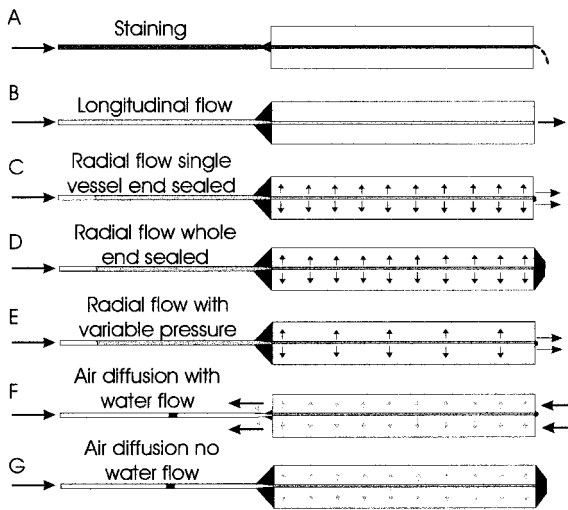


**Fig. 2.** Diagram outlining experimental methods used in this study: (A) staining of vessel walls; (B) determination of longitudinal conductivity—vessel end open; (C) determination of radial specific conductance—vessel end sealed, neighbouring vessels open; (D) determination of radial specific conductance—ends of all vessels sealed; (E) determination of bordered pit threshold pressures—vessel end sealed; water delivered with increasing pressure; (F) determination of gas diffusion from pressurized vessel—vessel end sealed, water flow present in neighbouring vessels; (G) determination of gas diffusion from pressurized vessel—ends of all vessels sealed, no water flow through neighbouring vessels.

a very low conductance. Thus,  $L_r$  describes the combined properties of this heterogeneous pathway.

#### Estimation of bordered pit pressure threshold

The degree to which air-filled bordered pits can contain positive pressures within individual conduits was assessed by determining the pressure dependence of radial water flow through previously air-filled vessels. A microcapillary was attached to a single vessel as described above (Fig. 1A, B, C), after which dry nitrogen gas was blown through the vessel at a pressure of 0.15 MPa for 10 min in an attempt to simulate conditions within an embolized vessel. The time of exposure to  $N_2$  gas was limited because of concerns of desiccating the surrounding tissues. The vessel was then refilled with water through the microcapillary at the same time as the open (distal) end of the vessel was observed using a stereo microscope. When water started to flow out of the vessel, the vessel end was immediately dried and sealed using acrylic glue. Positive pressures on the order of  $\sim 0.3$  MPa are needed to push water into gas-filled bordered pits of *F. americana* (Zwieniecki and Holbrook, 2000). Thus, it was expected that some of the bordered pits remained air-filled. The microcapillary was then connected to the pressure manifold and the flow rate into the stem was determined by monitoring the movement of the meniscus within the microcapillary (Fig. 2E). The applied pressure was increased in steps, starting at 0.1 MPa and increasing to 2.0 MPa. At each pressure step, three consecutive flow measurements were made to determine if a steady-state flow rate had been reached. Radial specific conductance was calculated for each delivery pressure as described above.

#### Gas movement from pressurized vessels

Gas diffusion through the tissue surrounding an individual xylem vessel was determined on stem segments that had been

vacuum infiltrated with de-ionized filtered water for 30 min to hydrate the stems. Microcapillary tubes were attached to an individual vessel as described above except that the microcapillary was sealed in such a way that no glue came into contact with any of the neighbouring vessels (Figs 1D, 2F). After the glue hardened ( $\sim 1$  min), safranin dye was pushed through the vessel, followed by dry  $N_2$  gas at a pressure of 0.4 MPa for 5 min to dry the interior of the vessel. The vessel lumen was then filled with air using a syringe and the open (distal) end of the vessel was sealed. A small droplet of water was inserted into the end of the microcapillary to provide an interface whose movement could be used to determine the flow rate of gas into the vessel. This water droplet also served to separate the air within the vessel from the  $N_2$  gas used to pressurize the microcapillary-vessel system. The microcapillary-vessel system was pressurized to 0.2 MPa and the movement of gas from the vessel determined by observing the movement of the meniscus in the microcapillary tube.

The rate at which gas was forced from a vessel was determined both when the water in adjacent vessels was stationary (all vessels sealed at either end; Fig. 2G) and when it was flowing (Fig. 2E). The latter allowed the importance of convection in the radial exchange of gases in woody stems to be estimated. Water movement through adjacent vessels was induced by attaching the branch segment to a hydraulic head (*c.* 2.5 kPa), resulting in a flow rate of approximately  $2 \text{ mg s}^{-1}$ .

It was assumed that gas exits the vessel by being forced into solution and then diffuses through the surrounding tissues to the outside air. An apparent diffusion coefficient ( $D$ ;  $\text{m}^2 \text{ s}^{-1}$ ) was calculated for the movement of gas across the stem based on a cylindrical geometry (Cussler, 1997):

$$D = \frac{j_{\text{gas}} r_o \ln(r_o/r_v)}{\Delta c_{\text{gas}}} \quad (5)$$

where  $j_{\text{gas}}$  is the flow rate of gas across the perimeter of the vessel ( $\text{mol m}^{-2} \text{ s}^{-1}$ ; calculated as the flow rate ( $\text{mol s}^{-1}$ ) into the sealed vessel divided by the interior surface area of the pressurized vessel ( $\text{m}^2$ )),  $r_v$  is the vessel radius (m),  $r_o$  is the radius of the outer boundary of the cylinder (m) which was assumed to be equal to the distance from the pressurized vessel to the nearest edge of the stem segment ( $\sim 1.0$  mm), and  $\Delta c_{\text{gas}}$  is the difference in concentration of dissolved gases in the water at the surface of the vessel and at the edge of the stem ( $\text{mol m}^{-3}$ ). Using Henry's Law,  $\Delta c_{\text{gas}}$  was calculated to determine the concentration of dissolved gases in equilibrium with the gas pressures existing in the pressurized vessel and at the edge of the stem. It was assumed that the volume fraction of nitrogen and oxygen in the gas phase was 0.8 and 0.2, respectively. The resulting Henry's Law constant was equal to  $7.75 \text{ e}^{-6} \text{ mol m}^{-3} \text{ Pa}^{-1}$ .

#### Leak tests

A critical aspect of this technique is the ability to make leak-proof seals both where the microcapillary is inserted into the vessel and at the distal end of the vessel. To test this, the microcapillary-vessel system was filled with either safranin dye or air and pressurized to 6 MPa. Stems in which the pressurized vessel was filled with air were submerged in water and a stereo-microscope was used to look for bubbles. Stems with vessels filled with safranin dye were pressurized for 1 h and then both ends of the stem were examined under the microscope for dye leakage at the point where the microcapillary was inserted into the vessel or at the wood/glue interface. Leak tests performed on 10 stems during protocol development demonstrated that it was possible to seal the microcapillary-vessel system completely.

During these experimental measurements, each stem was repeatedly checked for leaks. In the few cases (3 out of ~100) when a leak was observed, the sample was discarded.

## Results

### Vessel hydraulic properties

The measured longitudinal conductivity of single ash vessels followed the relationship predicted from the Poiseuille equation (Fig. 3). This was not surprising because ash has simple perforation plates and the vessel was continuous within the measured branch segment. Small deviations from the Poiseuille relation are likely to be the result of errors associated with determining vessel radii, longitudinal variation in vessel aperture, and the fact that vessels are never completely circular in cross-section.

The radial specific conductance measured with neighbouring vessels open at the distal end of the stem segment was  $2.26 \text{ e}^{-7} \text{ m MPa}^{-1} \text{ s}^{-1}$  ( $n=9$ ,  $SD=1.4 \text{ e}^{-7}$ ). When the neighbouring vessels were sealed at the distal end of the stem segment, the radial specific conductance was  $1.62 \text{ e}^{-7} \text{ m MPa}^{-1} \text{ s}^{-1}$  ( $n=12$ ;  $SD=1.1 \text{ e}^{-7}$ ). There was no significant difference between the two measures of radial flow ( $df=9$ ,  $t=0.64$  (dependent samples),  $P=0.53$ ). For these short segments, the radial specific conductance was approximately six orders of magnitude lower than the longitudinal conductance normalized by the cross-sectional area of the vessel lumen.

### Border pit pressure threshold

Radial specific conductance of vessels that had been flushed with dry nitrogen gas increased abruptly when the applied pressure exceeded  $\sim 0.4 \text{ MPa}$  (Fig. 4). Specific conductance increased significantly from an average initial value of  $3.2 \text{ e}^{-7} \text{ m MPa}^{-1} \text{ s}^{-1}$  to  $4.1 \text{ e}^{-7} \text{ m MPa}^{-1} \text{ s}^{-1}$  ( $df=4$ ;  $t=3.14$  (dependent samples),  $P=0.034$ ). The

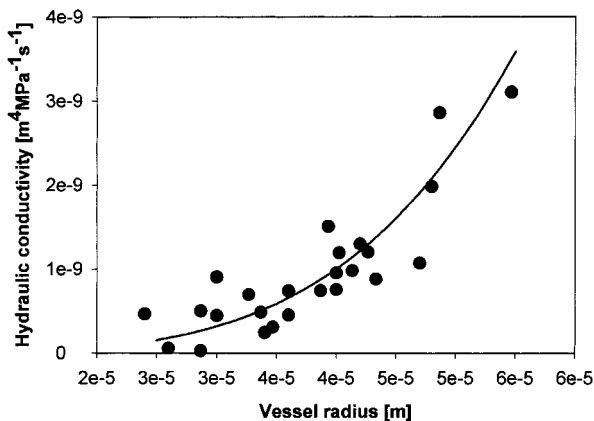


Fig. 3. Longitudinal conductivity of individual xylem vessels versus average vessel radius. Curve represents the conductivity calculated from the Poiseuille equation for flow in a circular conduit.

magnitude of the observed increase varied among the measured vessels. Prior to and after the threshold pressure was reached, specific conductance remained constant (Fig. 4). In one case, the pressure was increased and subsequently decreased in steps. In contrast to the observed step increase in radial specific conductance as the pressure was increased, radial specific conductance remained constant when the pressure was decreased (Fig. 4).

### Gas diffusion

The rate at which gas could be forced out through the sides of a pressurized vessel remained constant over a period of several hours (Fig. 5). When water was perfused through the neighbouring vessels, the calculated diffusion coefficient was  $4.18 \text{ e}^{-9} \text{ m}^2 \text{ s}^{-1}$  ( $n=3$ ,  $SD=1.28 \text{ e}^{-9}$ ). When there was no flow in the adjacent vessels, the calculated diffusion coefficient was  $2.95 \text{ e}^{-9} \text{ m}^2 \text{ s}^{-1}$  ( $n=7$ ,  $SD=5.28 \text{ e}^{-10}$ ). There was a significant difference between the two treatments ( $df=8$ ,  $t=2.35$ ,  $P=0.046$ ). The calculated diffusion coefficient was found to be of the same order of magnitude as the diffusion coefficient of air in water ( $1.95 \text{ e}^{-9} \text{ m}^2 \text{ s}^{-1}$ ; Yang and Tyree, 1992). Lack of complete agreement might result from the fact that cylindrical geometry assumed in these calculations oversimplifies the actual pathways by which gas exits the pressurized vessel.

The time necessary to displace the entire volume of the vessel was, on average, 1399 s when the water in adjacent vessels was static and 1026 s when water in adjacent vessels was flowing.

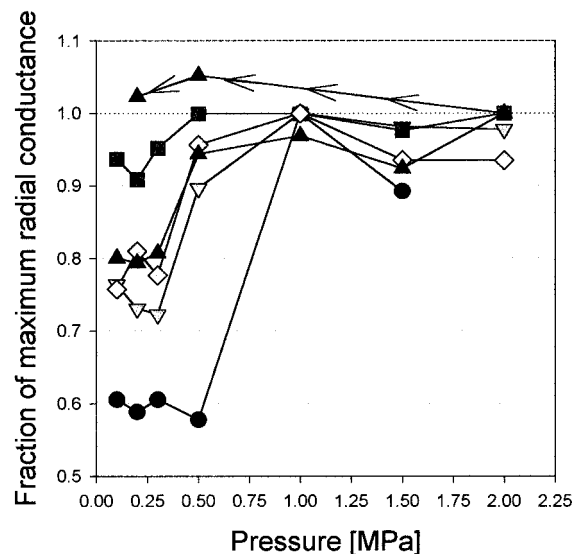


Fig. 4. Relative change in radial conductivity of individual vessels expressed as a fraction of maximum conductance as a function of increasing applied pressure (MPa). Each curve represents a different stem sample.

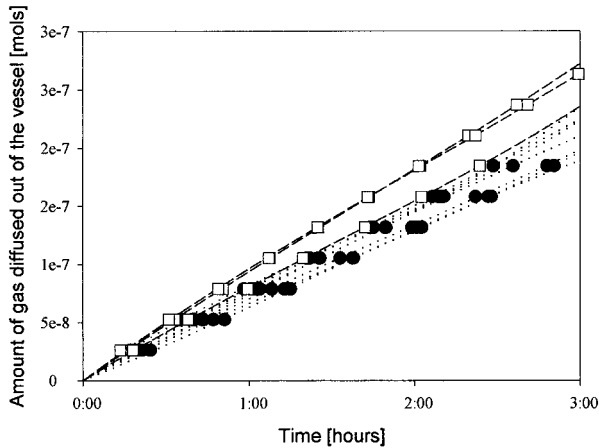


Fig. 5. Cumulative efflux of gas from a pressurized vessel (distal end blocked) versus time. Open symbols represents the situation when flow of water was present in surrounding vessels, closed symbols represent situation when there was no flow through the neighbouring vessels.

## Discussion

Previous attempts to compare measured hydraulic conductivity with values predicted from the Poiseuille equation (Münch, 1943; Tyree and Zimmermann, 1971; Giordano *et al.*, 1978; Woodhouse and Nobel, 1982; Calkin *et al.*, 1984) indicate that the Poiseuille equation significantly overestimates the hydraulic conductivity of xylem vessels. In contrast, good agreement was found between theoretical calculations of hydraulic conductivity and measurements of individual vessels in ash stems. Because ash has simple perforation plates, it would be expected to behave like an ideal pipe. In addition, short stem segments were used to remove any effect of water flow through inter-vessel pits. This agreement was interpreted as evidence that the single vessel technique is capable of accurately measuring the longitudinal conductivity of individual vessels. This suggests that further measurements using this technique will be useful in determining the additional resistance imposed by vessel endings (i.e. where water is forced to flow through bordered pits), as well as to compare the effects of different perforation plate structures, warty layers, or pit geometry (size, ornamentation). As far as the authors are aware, there is only one other study in which the hydraulic properties of individual vessels were measured (Giordano *et al.*, 1978). They report a significant discrepancy between measurements of the longitudinal conductivity of cucumber vessels with values predicted from the Poiseuille equation. Although Cucurbitaceae are known for having long vessels, the authors did not confirm that they were in an open vessel and thus the discrepancy could be due to the presence of vessel end walls. It was

also noted that the single vessel technique must be applied with great care. In particular, it was noted that in many of these preliminary trials the capillary tips were prone to blockage if they were not seated properly in the vessel lumen, resulting in extremely high resistances.

The single vessel technique allows, for the first time, an investigation of factors influencing radial movement of gas and water. Water flow through the lateral walls of xylem vessels may occur through several parallel pathways, including water movement through the thick secondary walls and through pits connecting the vessel with adjacent cells. The measurements made in this study cannot distinguish between these different pathways. The overall conductance for radial water movement in *F. americana* vessels is small compared to the longitudinal conductance, although it is difficult to evaluate the significance of this value, as no comparable measurements exist for single vessels in this or other species. However, bulk values of liquid permeability in the transverse direction through timber are similar in magnitude to those measured in this study (Siau, 1984).

Radial specific conductance sets the minimum rate of water inflow needed to refill an embolized vessel. For refilling to occur, water must be pumped into the gas-filled conduit at a rate exceeding leakage through the vessel perimeter. The rate at which water would leak through the radial walls of a 100  $\mu\text{m}$  diameter vessel subject to a pressure difference of 1 MPa between the refilling vessel and surrounding tissue is  $1.9 \text{ e}^{-4} \text{ mm}^3 \text{ s}^{-1}$  per mm of vessel length. This estimate was made using measurements of radial specific conductance of fully hydrated vessels in which all lateral pathways are able to conduct water and, thus, may substantially overestimate water outflow during refilling. Specifically, during refilling, the water flow through bordered pits may be blocked by the presence of gas trapped in the pit chamber (Holbrook and Zwieniecki, 1999).

The existence of a non-zero ( $\sim 50^\circ$ ) contact angle of water on vessel walls and the flared opening into the bordered pit chamber should result in the formation of a convex gas:water interface (Zwieniecki and Holbrook, 2000). Because of the high surface tension of water, this interface will prevent water from filling the pit chamber unless the threshold pressure required to expand this interface is exceeded. At present, there is no method to observe conditions within the bordered pits of a refilling vessel directly. However, measurements of radial specific conductance in relation to applied pressure in air-dried vessels demonstrate a step increase at  $\sim 0.4$  MPa. This value is similar to the pressure threshold calculated from measurements of pit geometry and contact angle for *F. americana* (0.3 MPa; Zwieniecki and Holbrook, 2000). The magnitude of the change was less than had been anticipated. It is possible that the pre-treatment to remove water from the bordered pits was only partially successful

and thus that some fraction of the bordered pits remained hydraulically connected to surrounding tissues.

When a vessel cavitates it is initially filled with water vapour. The rate at which the lumen becomes air-filled is set by the rate at which air can diffuse through surrounding tissues. To reverse this process (i.e. for refilling to occur), all of this air must be removed from the vessel. This presumably happens due to the existence of positive pressures that force the gas into solution, allowing it to diffuse away towards the edge of the stem or be carried away with the transpiration stream. Thus, both embolism formation and refilling depend upon the rate at which air can diffuse across surrounding tissues. The diffusion coefficient for air through stem tissues estimated in this study is within the same order of magnitude as the diffusion of air through water (Lide, 1995). These measurements of the rate of air movement from a pressurized vessel shows that the time needed to replace the total volume of gas within an ash vessel is approximately 20 min under applied conditions. This measured value is less than those estimated by the modelling study of Yang and Tyree (Yang and Tyree, 1992). Their estimate of time to refill a 50 µm diameter air-filled vessel in a 1 mm diameter stem (pressure within the vessel equal to 150 kPa) was approximately 2 h (Yang and Tyree, 1992), exceeding the time measured in this study even if corrected for the vessel diameter and applied pressure. This does not mean that refilling actually takes place this fast due to limitations on the rate at which water can be pumped into the vessel. These data, however, indicate that gas diffusion is not a major factor limiting the rate of refilling. It was also found that flow in neighbouring conduits increased the rate at which gas could be lost from a pressurized vessel. However, the effect of convection on the time needed for gas removal was small.

In this paper, as far as is known, the first direct measurements of radial hydraulic properties and gas diffusion coefficient estimates across the perimeter of an individual xylem vessel are presented. This technique shows great promise for increasing the understanding of structure–function relations of xylem conduits. In particular, it provides a new tool for exploring the hydraulic implications of the substantial interspecific variation in wood anatomy among vascular plants (Esau, 1977; Zimmermann, 1983). In addition, direct measurements of radial transport properties may help in understanding the mechanism by which embolized vessels are refilled. Although the estimates of radial specific conductance for ash suggest that refilling of cavitated vessels during periods of transpiration might be difficult due to water efflux through the vessel perimeter, more detailed studies are required to separate water flow through bordered pits from movement across the wall itself. On the other hand, estimates of gas diffusion suggest that gas removal is not a significant constraint on the refilling process.

## Acknowledgements

This work was supported by USDA competitive research grant 98-35100-6081, and the Andrew W Mellon Foundation. We wish to thank MJ Burns, AR Cobb, TS Feild, R Spicer, and MV Thompson for helpful comments on the manuscript.

## References

- Alder N, Sperry J, Pockman W. 1996. Root and stem xylem embolism, stomatal conductance, and leaf turgor in *Acer grandidentatum* populations along a soil moisture gradient. *Oecologia* **105**, 293–301.
- Calkin H, Gibson A, Nobel P. 1984. Xylem water potential and hydraulic conductances in eight species of ferns. *Canadian Journal of Botany* **63**, 632–637.
- Canny MJ. 1997. Vessel contents during transpiration—embolism and refilling. *American Journal of Botany* **84**, 1223–1230.
- Cochard H, Ewers FW, Tyree MT. 1994. Water relations of tropical vine-like bamboo (*Rhipidocladum recemiflorum*): root pressures, vulnerability to cavitation and seasonal changes in embolism. *Journal of Experimental Botany* **45**, 1085–1089.
- Cussler EL. 1997. *Diffusion, mass transfer in fluid systems*. New York: Cambridge University Press, 580.
- Edwards W, Jarvis P, Grace J, Moncrieff J. 1994. Reversing cavitation in tracheids of *Pinus sylvestris* L. under negative water potentials. *Plant, Cell and Environment* **17**, 389–397.
- Esau K. 1977. *Anatomy of seed plants*. New York: John Wiley & Sons, 550.
- Giordano R, Salleo A, Salleo S, Wanderlingh F. 1978. Flow in xylem vessels and Poiseuille's law. *Canadian Journal of Botany* **56**, 333–338.
- Holbrook NM, Zwieniecki MA. 1999. Xylem refilling under tension. Do we need a miracle? *Plant Physiology* **120**, 7–10.
- Jarbeau J, Ewers F, Davis S. 1995. The mechanism of water-stress-induced embolism in two species of chaparral shrubs. *Plant, Cell and Environment* **18**, 189–196.
- Kockenberger W, Pope JM, Xia Y, Jeffrey KR, Komor E, Callaghan PT. 1997. A non-invasive measurement of phloem and xylem water flow in castor bean seedlings by nuclear magnetic resonance microimaging. *Planta* **201**, 53–63.
- Lide DR. 1995. *CRC handbook of chemistry and physics*. London: CRC Press.
- Magnani F, Borghetti M. 1995. Interpretation of seasonal changes of xylem embolism and plant hydraulic resistance in *Fagus sylvatica*. *Plant, Cell and Environment* **18**, 689–696.
- Milburn J. 1979. *Water flow in plants*. London: Longman, 225.
- Milburn J, McLaughlin M. 1974. Studies of cavitation in isolated vascular bundles and whole leaves of *Plantago major* L. *New Phytologist* **73**, 861–871.
- Münch E. 1943. Durchlässigkeit der siebrohren für druckstromen. *Flora (Jena, 1818–1965)* **136**, 223–262.
- O'Leary J. 1965. Root-pressure exudation in woody plants. *Botanical Gazette* **126**, 108–115.
- Pickard WF. 1989. How might a tracheary element which is embolized by day be refilled by night? *Journal of Theoretical Biology* **141**, 259–279.
- Putz F. 1983. Leaf biomass and leaf area of a 'terra firme' forest in the Rio Negro Basin, Venezuela. *Biotropica* **15**, 185–189.
- Salleo S, LoGullo M, DePaoli D, Zippo M. 1996. Xylem recovery from cavitation-induced embolism in young plants of *Laurus nobilis*—a possible mechanism. *New Phytologist* **132**, 47–56.
- Siau JF. 1984. *Transport processes in wood*. New York: Springer-Verlag, 245.

- Sperry J.** 1986. Relationship of xylem embolism to xylem pressure potential, stomatal closure and shoot morphology in the palm *Rhapis excelsa*. *Plant Physiology* **80**, 110–116.
- Sperry JS, Donnelly JR, Tyree MT.** 1988a. A method for measuring hydraulic conductivity and embolism in xylem. *Plant, Cell and Environment* **11**, 35–40.
- Sperry J, Donnelly J, Tyree M.** 1988b. Seasonal occurrence of xylem embolism in sugar maple (*Acer saccharum*). *American Journal of Botany* **75**, 1212–1218.
- Sperry JS, Alder NN, Eastlack SE.** 1993. The effect of reduced hydraulic conductance on stomatal conductance and xylem cavitation. *Journal of Experimental Botany* **44**, 1075–1082.
- Sperry J, Ikeda T.** 1997. Xylem Cavitation in roots and stems of douglas-fir and white fir. *Tree Physiology* **17**, 275–280.
- Tyree M, Zimmermann M.** 1971. The theory and practice of measuring transport coefficients and sap flow in the xylem of red maple stems (*Acer rubrum*). *Journal of Experimental Botany* **22**, 1–18.
- Tyree MT, Ewers FW.** 1991. The hydraulic architecture of trees and other woody plants. *New Phytologist* **119**, 345–360.
- Tyree MT, Yang S.** 1992. Hydraulic conductivity recovery versus water pressure in xylem of *Acer saccharum*. *Plant Physiology* **100**, 669–676.
- Tyree MT, Salleo S, Nardini A, Lo Gullo MA, Mosca R.** 1999. Refilling of embolized vessels in young stems of laurel. Do we need a new paradigm? *Plant Physiology* **120**, 11–21.
- Waring R, Running S.** 1978. Sapwood storage: contribution to transpiration and effect upon water conductance through the stems of old growth Douglas-fir. *Plant, Cell and Environment* **1**, 131–140.
- Woodhouse R, Nobel P.** 1982. Stipe anatomy, water potentials and xylem conductances in seven species of ferns (Filicopsida). *American Journal of Botany* **69**, 135–140.
- Yang S, Tyree MT.** 1992. A theoretical model of hydraulic conductivity recovery from embolism with comparison to experimental data on *Acer saccharum*. *Plant, Cell and Environment* **15**, 633–643.
- Zimmermann M, Brown C.** 1971. *Trees: structure and function*. New York: Springer-Verlag, 336.
- Zimmermann MH.** 1983. *Xylem structure and the ascent of sap*. Berlin: Springer-Verlag, 143.
- Zwieniecki MA, Holbrook NM.** 1998. Short term changes in xylem water conductivity in white ash, red maple and sitka spruce. *Plant, Cell and Environment* **21**, 1173–1180.
- Zwieniecki MA, Holbrook NM.** 2000. Bordered pit structure and vessel wall surface properties—implications for embolism repair. *Plant Physiology* **123**, 1015–1020.
- Zwieniecki MA, Hutrya L, Thompson MV, Holbrook NM.** 2000. Dynamic changes in petiole specific conductivity in red maple (*Acer rubrum* L.), tulip tree (*Liriodendron tulipifera* L.) and northern fox grape (*Vitis labrusca* L.). *Plant, Cell and Environment* **23**, 407–414.